

## Improving the Delivery of Radionuclides for Imaging and Therapy of Cancer Using Pretargeting Methods

Robert M. Sharkey,<sup>1</sup> Habibe Karacay,<sup>1</sup> Thomas M. Cardillo,<sup>2</sup> Chien-Hsing Chang,<sup>3</sup> William J. McBride,<sup>2</sup> Edmund A. Rossi,<sup>3</sup> Ivan D. Horak,<sup>2</sup> and David M. Goldenberg<sup>1</sup>

**Abstract** The article reviews the background and current status of pretargeting for cancer imaging and therapy with radionuclides. Pretargeting procedures were introduced ~20 years ago as an alternative to directly radiolabeled antibodies. Because they were multistep processes, they were met with resistance but have since progressed to simple and improved procedures that could become the next generation of imaging and therapy with radionuclides. The separation of the radiolabeled compound from the antibody-targeting agent affords pretargeting procedures considerable flexibility in the radiolabeling process, providing opportunities for molecular imaging using  $\gamma$ - or positron-emitting radionuclides and a variety of  $\beta$ - and  $\alpha$ -emitting radionuclides of therapeutic applications. Pretargeting methods improve tumor/nontumor ratios, exceeding that achieved with directly radiolabeled Fab' fragments, particularly within just a few hours of the radionuclide injection. In addition, tumor uptake exceeds that of a Fab' fragment by as much as 10-fold, giving pretargeting a greatly enhanced sensitivity for imaging. Advances in molecular biology have led to the development of novel binding proteins that have further improved radionuclide delivery in these systems. Studies in a variety of hematologic and solid tumor models have shown advantages of pretargeting compared with directly radiolabeled IgG for therapy, and there are several clinical studies under way that are also showing promising results. Thus, the next generation of targeting agents will likely employ pretargeting approaches to optimize radionuclide delivery for a wide range of applications.

Radiation continues to play an integral role in the management of cancer, from the use of X-rays and computed tomography for detection to the use of external beam and interstitial radiotherapy (brachytherapy and rapid interstitial therapy) for treatment. Nuclear medicine, which involves the use of internally administered radionuclides, traditionally has played a minor role in the management of cancer, initially relying primarily on the use of [<sup>67</sup>Ga]citrate for lymphoma imaging and <sup>131</sup>I Na for thyroid cancer treatment. However, with the advent of positron emission tomography and [<sup>18</sup>F]deoxyglucose, and thanks to the development of new antibody-guided therapeutics for non-Hodgkin's lymphoma and emerging peptide-targeted therapeutics, the role of

nuclear medicine in the management of cancer is increasing (1, 2).

Except for <sup>131</sup>I Na and radionuclides used for palliation of bone pain that are selectively taken up by their respective tissues, the specificity for cancer of internally administered radionuclides depends on its coupling to a targeting compound. For example, [<sup>18</sup>F]deoxyglucose is concentrated in cancers because they are more metabolically active than most other cells in the body and therefore will accrue more deoxyglucose than surrounding cells. Antibodies have been one of the most commonly used targeting agents, with an extensive history spanning over 50 years (3). During this time, there has been substantial progress in identifying new cancer markers and in applying molecular biology and engineering to improve the design, affinity, and reduced immunogenicity of antibodies used in targeting (3). However, the direct attachment of a radionuclide to the large IgG molecule can limit both imaging and therapeutic applications. With a molecular weight of 150,000 Da, IgG clears slowly from the blood. Slow blood clearance has been identified as a major impediment for tumor localization, with preclinical and clinical studies showing that visualization was only possible if imaging were delayed for ~7 days or if blood-pool activity was subtracted from the images (4, 5). For therapeutic applications, the slow clearance of radioactivity from the blood continually exposes the red marrow to radiation, resulting in dose-limiting myelotoxicity. Whereas the radiation-absorbed dose delivered at the maximum tolerated dose for radiolabeled IgG is

**Authors' Affiliations:** <sup>1</sup>Center for Molecular Medicine and Immunology, Belleville, New Jersey; <sup>2</sup>Immunomedics, Inc. and <sup>3</sup>IBC Pharmaceuticals, Inc., Morris Plains, New Jersey

**Grant support:** Office of Science (Biological and Environmental Research), U.S. Department of Energy grant DE-FG02-95ER62028 (R.M. Sharkey), USPHS grant EB002114 from the National Institute for Biomedical Imaging and Bioengineering (R.M. Sharkey), and Thomas and Agnes Carvel Foundation grant (Garden State Cancer Center).

Presented at the Tenth Conference on Cancer Therapy with Antibodies and Immunoconjugate, October 21-23, 2004, Princeton, New Jersey.

**Requests for reprints:** Robert M. Sharkey, Center for Molecular Medicine and Immunology, 520 Belleville Avenue, Belleville, NJ 10709. Phone: 973-844-7121; Fax: 973-844-7020; E-mail: rmarsharkey@gscancer.org.

© 2005 American Association for Cancer Research.  
doi:10.1158/1078-0432.CCR-1004-0009

sufficient to result in clinically significant antitumor effects in non-Hodgkin's lymphoma, for solid tumors the total radiation dose will likely need to be increased by at least 2.5-fold what is achieved currently with the maximally administered activities. A variety of techniques, including using smaller antibody fragments (6) or of clearing methods, such as a second antibody (7) or extracorporeal immunoadsorption (8, 9), have been applied to reduce the amount of radiolabeled antibody from the blood, thereby permitting higher administered activities, but each of these methods has certain limitations. For example, by accelerating the blood clearance, the proportion of radioactivity delivered to the tumor [i.e., percent injected dose per gram (%ID/g)] is lowered substantially with antibody fragments. Although the administered activity is increased, it is not always possible to compensate for the proportional loss in uptake and increase the total amount of radioactivity delivered to the tumor. In addition, when coupled to a radiometal, antibody fragments <60,000 Da can have as much as 10 to 20 times more radioactivity retained in the kidneys than in the tumor (10). Because radioiodine is not retained by the kidneys, antibody fragments may be restricted to using radioiodine, although there have been reports of successful therapy with antibody fragments radiolabeled directly with radiometals (11).

Rather than directly coupling the radionuclide to an antibody or its fragments, pretargeting methods that separate the antibody from the radionuclide targeting seem to address many of the limitations of the direct approach by (a) using smaller molecular weight carriers for the radionuclide that are rapidly cleared from the blood (within minutes) and body; (b) allowing the radionuclide carrier to be more easily radiolabeled with any number of radionuclides to a high specific activity and without compromising binding; (c) targeting the same or even higher levels of radioactivity to tumors as with a directly radiolabeled IgG; (d) affording extremely rapid tumor uptake (within minutes), thereby increasing the radiation-absorbed dose rate to the tumor; (e) significantly increasing tumor/nontumor ratios with tumor uptake exceeding activity in the blood by as much as 10:1 or more within 1 hour; and (f) reducing the amount of radioactivity in the kidneys 10- to 20-fold over that seen with a radiometal-labeled antibody fragment.

The concept of separating the radionuclide from the antibody as a means of targeting radionuclides was first proposed by Reardan et al. (12), who, after showing that specific antibodies could be prepared to metal chelates, proposed that it might be possible to prepare antibodies with dual specificity to tumor-associated antigens and to the metal chelate. This novel concept essentially set the stage for the development of pretargeting strategies based on bispecific antibodies (13-15) but also spawned the development of another innovative pretargeting strategy that used streptavidin or avidin in conjunction with biotin (16). In addition to radionuclides, antibody-directed enzyme-prodrug therapy (17) is another form of pretargeting that itself has been responsible for generating several new pretargeting initiatives, such as gene-directed enzyme-prodrug therapy (18), polymer-directed enzyme-prodrug therapy (19), and antibody-targeted, triggered, electrically modified prodrug-type strategy (20).

At the core of all pretargeting systems is the minimum requirement for a two-component targeting system. The first component given is not tagged with a radionuclide, but instead

has the primary purpose of (a) seeking out and binding to a unique binding site (e.g., tumor-associated antigens) and (b) having the capacity to also bind the small molecular weight carrier on which the radionuclide is attached. Thus, the primary targeting agent and the radionuclide must share a common recognition system. Nature is replete with a variety of recognition systems, such as enzyme-substrates (used by the prodrug pretargeting methods), receptor-ligand, and antibody-hapten (such as antimetal chelate antibodies and chelates loaded with radiometals) that could be used for this purpose. However, because the recognition system must have a restricted expression in normal tissues, this has greatly limited the use of many naturally occurring recognition systems to the extent that, for radionuclide targeting, there are currently two pretargeting models that have been extensively examined, but there is also a third model currently under investigation. One model relies on the ultra-high affinity of streptavidin for biotin. This model, first introduced by Hnatowich et al. (16), can be depicted in several ways, but two configurations have been reported most frequently. In one approach, commonly called a two-step method (Fig. 1), streptavidin is coupled to an antitumor IgG (streptavidin-IgG) making a ~210-kDa conjugate. Streptavidin (bacterial origin and nonglycosylated) and avidin (primarily derived from hen eggs and glycosylated) are composed of four subunits, with each subunit capable of binding a single biotin with a dissociation constant of  $\sim 10^{-15}$  mol/L (~6 logs higher than most antigen-antibody interactions). The unlabeled streptavidin-IgG is administered first, and then once it has achieved a maximum uptake in the tumor (e.g., 1-3 days), radiolabeled biotin is administered. Because the streptavidin-IgG clears so slowly from the blood, if given at this time, the radiolabeled biotin would bind to the streptavidin-IgG in the blood and tissues, preventing a sizeable portion of the radiolabeled biotin from reaching the tumor. Indeed, with such a high affinity for biotin, even a small amount of conjugate in the blood and tissues would bind the biotin irreversibly. The solution to this dilemma was to have an agent that could quickly remove the conjugate from the blood once it had achieved maximum tumor uptake. The first agent developed for this was a conjugate composed of human serum albumin coupled with biotin that would not only serve as the recognition unit to bind the streptavidin-IgG but also could simultaneously block subsequent biotin binding. To prevent the human serum albumin-biotin conjugate from competing for the radiolabeled biotin's binding to the streptavidin-IgG localized in the tumor, galactose was coupled to human serum albumin-biotin conjugate so that it would be readily recognized by hepatocytes and removed from the blood (21). Thus, this two-step method incorporates an additional step to remove the streptavidin-IgG conjugate from the blood before administering the radiolabeled biotin. A period of several hours, but typically 1 to 2 days, is given to allow for the streptavidin-IgG clearance to occur before the radiolabeled biotin is given. As mentioned earlier, a prerequisite for pretargeting is that the recognition system must not be prevalent in critical normal tissues. Biotin is quite abundant in normal tissues, because it is an essential cofactor for several enzymes (22); thus, a streptavidin-IgG conjugate can be predisposed to the binding of endogenous biotin before the radiolabeled biotin is given (23). Fortunately, levels of free biotin in humans have been reported to be lower than in many

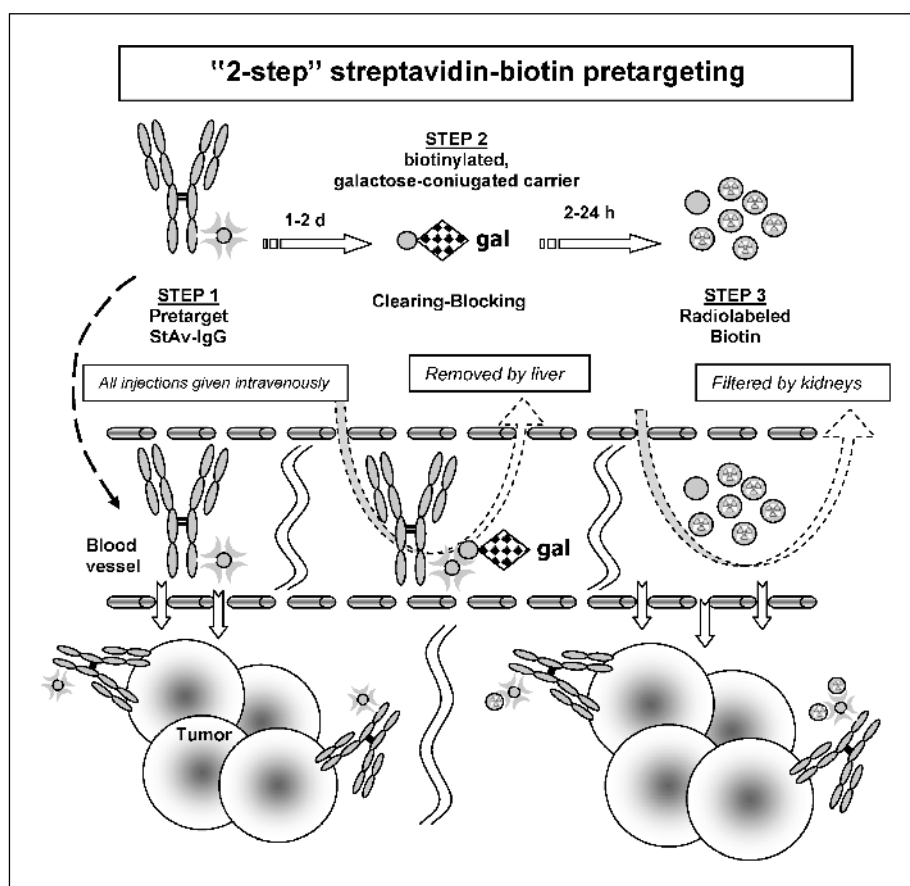


**Fig. 1.** Schematic representation of the "two-step" streptavidin-biotin pretargeting procedure. An antitumor IgG-streptavidin conjugate is given i.v. to localize to the tumor. After 1 to 2 days to allow for maximum tumor accretion, a clearing agent is used to quickly remove the conjugate from the blood, transporting it to the liver to be processed before radiolabeled biotin is given.

other animals (24); thus, the level of biotin binding by a streptavidin conjugate does not seem to be compromised in patients (23, 25); however, mice have substantial stores of assessable biotin, making it necessary when examining streptavidin-IgG conjugates to place mice on a biotin-deficient diet for several days before administering the conjugate to optimize tumor localization of the radiolabeled biotin (26).

The other variation of the streptavidin-biotin pretargeting systems (Fig. 2) has been called a three-step approach (27). This method starts with a biotinylated antitumor antibody; however, rather than using radiolabeled streptavidin or avidin that would have unwanted accretion in normal tissues (28), the method uses an intermediary injection of avidin to bind to the IgG-biotin in the blood, and because avidin is glycosylated, the complex will be cleared rapidly to the liver. Streptavidin is then given, which can then bind to the tumor-bound IgG-biotin. After a suitable waiting period is given to clear the streptavidin and avidin from the blood, the radiolabeled biotin is given, and because streptavidin is multivalent, a bridge is formed between the tumor-bound IgG-biotin and the radiolabeled biotin vis-à-vis the streptavidin.

A new model being investigated for pretargeting involves the use of complementary oligonucleotides (Fig. 3). Different types of oligonucleotides have been examined; however, more recently, morpholino oligomers have been used because of their enhanced stability to nucleases (29). An attractive feature of this model is the potential for multiple binding sites of the radiolabeled morpholino compound to the complementary morpholino strand pretargeted to a tumor by an antibody.

This model is in early preclinical testing and has had some promising initial results (29–32).

The third model (Fig. 4) is based on the use of a bispecific monoclonal antibody (mAb) as originally proposed by Reardan et al. (12). One arm of the bispecific mAb is specific for a tumor marker, whereas most often the other arm is against a chelated metal (33–37). The bispecific mAb has usually been prepared by chemically coupling the Fab' of the antitumor mAb to the Fab' of the anti-chelate-metal mAb, although bispecific mAb IgG prepared from a quadroma and molecularly engineered bispecific mAb have also been used (36, 38). Recombinant bispecific mAb are particularly attractive not only from the perspective of ease of production (only one cell line and one product need to be made) but also because their molecular size is approximately half the size as the conventionally used Fab' × Fab' chemical conjugates, giving these constructs a distinct pharmacokinetic advantage (38). In addition, constructs can be prepared with divalent binding capability to the target tumor antigen and still be smaller in size than a Fab' × Fab' bispecific mAb (38, 39). Rossi et al. (39) reported that this type of construct might have an advantage for pretargeting based on its higher uptake in tumors measured at a time when the blood concentration for this construct and a Fab' × Fab' bispecific mAb were the same. In preclinical and clinical practice, the bispecific mAb pretargeting methods have been used highly successfully without relying on a clearing step. Instead, a period of 1 to 7 days is given to allow the bispecific mAb to clear naturally from the blood before administering the radiolabeled hapten.

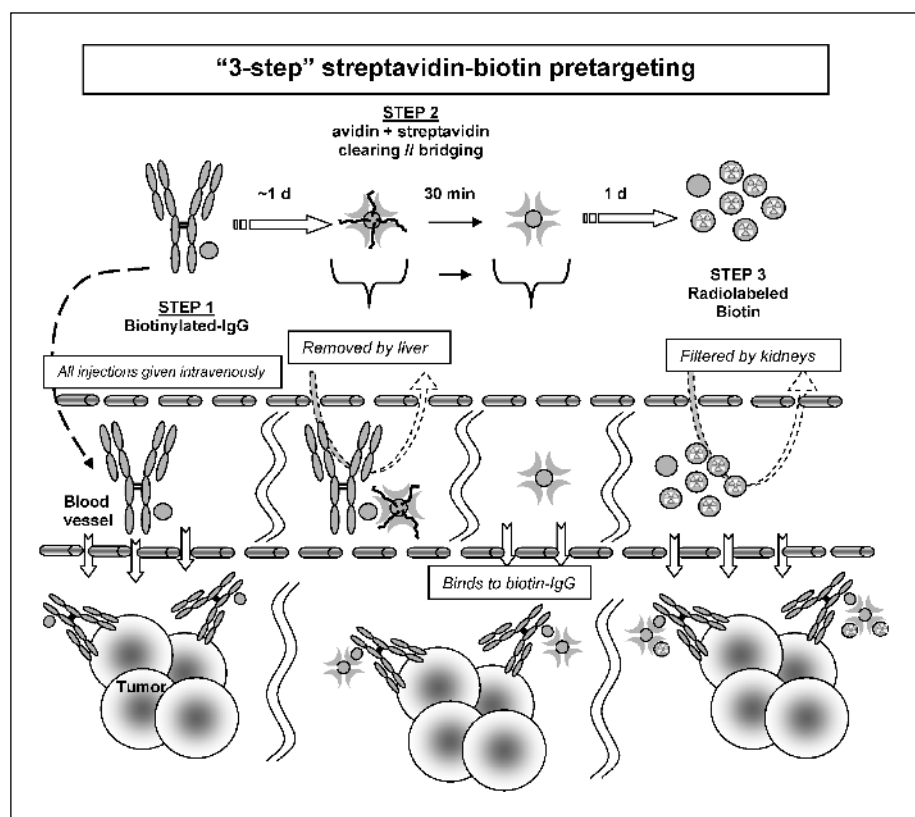


**Fig. 2.** Schematic representation of the three-step streptavidin-avidin-biotin pretargeting procedure. A biotin-conjugated antitumor IgG is given i.v. and allowed to localize to the tumor. In the next step, the naturally glycosylated avidin is given, which rapidly clears IgG-biotin from the blood for processing in the liver. Soon after the avidin injection, streptavidin is given. Streptavidin entering the tumor vascular bed will bind to the biotin-conjugated IgG, with the remaining material itself cleared from the body by renal filtration. Finally, radiolabeled biotin is given, and it will bind to the multivalent streptavidin that acts as a bridge between the tumor-bound biotin-IgG and the radiolabeled biotin.

Although this does not ensure that the radiolabeled hapten is administered when the uptake of the bispecific mAb in the tumor is at its highest level, the %ID/g of the radiolabeled product captured in the tumor by a bispecific mAb pretargeting procedure can also equal the maximum uptake of a directly radiolabeled antibody in a similar manner as a streptavidin-IgG pretargeting procedure (40). This is because a sufficient amount of bispecific mAb is given to create a molar excess of bispecific mAb in the tumor compared with the amount of peptide that will ultimately become accessible for capture. A commonly held belief for all pretargeting procedures is that the primary targeting agent should be given in exceedingly large doses to maximize the number of surrogate binding sites within the tumor to capture radiolabeled compound. Our experience has shown that the optimum dose level for the bispecific mAb is determined by the moles of the radiolabeled compound given in association with the radioactivity dose; therefore, it need not be an excessive amount (40). Indeed, Kraeber-Bodere et al. (41) have shown 40 mg/m<sup>2</sup> with a 5-day interval to be optimal for a Fab' × Fab' bispecific mAb in patients used in conjunction with an <sup>131</sup>I-labeled hapten. Because another important aspect for all pretargeting procedures is for the radiolabeled compound to be prepared at the highest possible specific activity, it is generally possible to use far less of the primary targeting agent than would be required to saturate the target antigen in most tumors.

Another advantage for pretargeting is that the compounds used in most pretargeting procedures are much more resilient to radiolabeling conditions than antibodies, which can result in an increase in the specific activity of the radiolabeled

compound, and may even allow for a wider range of radionuclides to be examined. For example, with the particular peptide-haptens we have used, a specific activity of 1,600 Ci <sup>90</sup>Y/mmol is possible without the need for purification, because >98% of the radionuclide are bound to the 1,4,7,10-tetraazacyclododecane-*N,N',N'',N'''*-tetraacetic acid (DOTA)-peptide-hapten (42). At this specific activity, ~1 in every 30 peptide-hapten molecules is radiolabeled. This compares with a specific activity of only ~745 Ci/mmol for <sup>90</sup>Y-DOTA-IgG (at 5 mCi <sup>90</sup>Y/mg IgG). With ultrapure, high-specific activity <sup>177</sup>Lu, we have been able to achieve specific activities of ~4,000 Ci/mmol, again without the need for purification, with 1 in every 5 peptide-haptens radiolabeled.<sup>4</sup>

Most of the anti-chelate-metal antibodies have nanomolar affinities, and in several instances, the metal chelate-binding arm of the bispecific mAb is more avidly bound to the specific chelate-metal complex used to prepare the anti-chelate-metal mAb. This high level of specificity can restrict the utility of a bispecific mAb to only a limited number of chelate-metal complexes. An alternate approach would use an anti-hapten antibody that is directed against a small compound that is not directly responsible for binding the radionuclide. Janevik-Ivanovska et al. (43) first reported an example of this using an antibody directed against histamine-succinyl glycine (HSG). We have shown that bispecific mAbs prepared with this anti-HSG antibody can be used in conjunction with short peptides that incorporate two HSG moieties (42). The peptide sequence serves as coupling sites where chelates, such as DOTA (used to

<sup>4</sup> Unpublished data.

chelate  $^{111}\text{In}$ ,  $^{90}\text{Y}$ ,  $^{177}\text{Lu}$ , and  $^{67}\text{Ga}$ ), or even a  $^{99\text{m}}\text{Tc}$ -binding moiety can be bound, allowing flexibility in the types of radionuclides that can be used with this pretargeting system. The peptide core can also be varied to alter the distribution of the radiolabeled peptide-HSG-hapten so that it is cleared primarily by urinary excretion (42).

A key component of a bispecific mAb pretargeting system is the valency of the hapten. Le Doussal et al. (35) discovered that divalent haptens are retained better than monovalent haptens, because in this configuration two bispecific mAbs that are typically monovalently bound to the tumor antigen can be cross-linked. This process is called an affinity enhancement system. Others have confirmed the superiority of divalent haptens (36, 44); therefore, all peptide-haptens used in pretargeting procedures have since incorporated two haptens for bispecific mAb recognition. There is also evidence that divalency of the bispecific mAb may further enhance uptake and retention of the radiolabeled compound (45).

Although the high affinity of streptavidin for biotin might lead one to believe that a streptavidin pretargeting procedure would have an advantage for pretargeting compared with the lower affinity of a bispecific mAb pretargeting system, in reality both systems require stable binding to the tumor. Thus, the affinity/avidity of the primary targeting antibody agent to the tumor would likely define the uptake and longevity of binding of the radiolabeled compound. A review of the uptake and normal tissue distribution data reported by the various groups using these different methods suggests that each would likely provide similar uptake and retention of radiolabeled product. Although the slow blood clearance of

the streptavidin-IgG or even recombinant single-chain Fv-streptavidin constructs is one reason a clearing agent is used with this procedure, it is also likely that the ultrahigh affinity of streptavidin-avidin for biotin is indispensable, because even a small amount of these agents remaining in the blood would likely result in the binding of a sizable portion of the radiolabeled biotin, whereas the lower affinity of the bispecific mAb system might reduce the prospect that the radiolabeled hapten forms stable complexes with the bispecific mAb in the blood. A disadvantage for procedures using streptavidin is its immunogenicity, which would reduce the possibility for using these procedures on multiple occasions, whereas bispecific antibodies can be fully humanized to reduce their immunogenicity. Regardless of the pretargeting procedure one elects to use, there is considerable experience in the literature, indicating their superiority for targeting radionuclides.

### Pretargeting for Improved Imaging

The difficulty caused by the slow clearance of a directly radiolabeled IgG in allowing for clear visualization of tumors was evident in some of the earliest imaging studies (4). Initial clinical success in cancer imaging came primarily because of the use of computer-aided subtraction techniques that were used to distinguish between radioactivity in a given tissue or region that could be attributed to radioactivity in the blood compared with specific accretion in the tumor (5), but later it was shown that earlier visualization could be achieved with antibody fragments because of their more

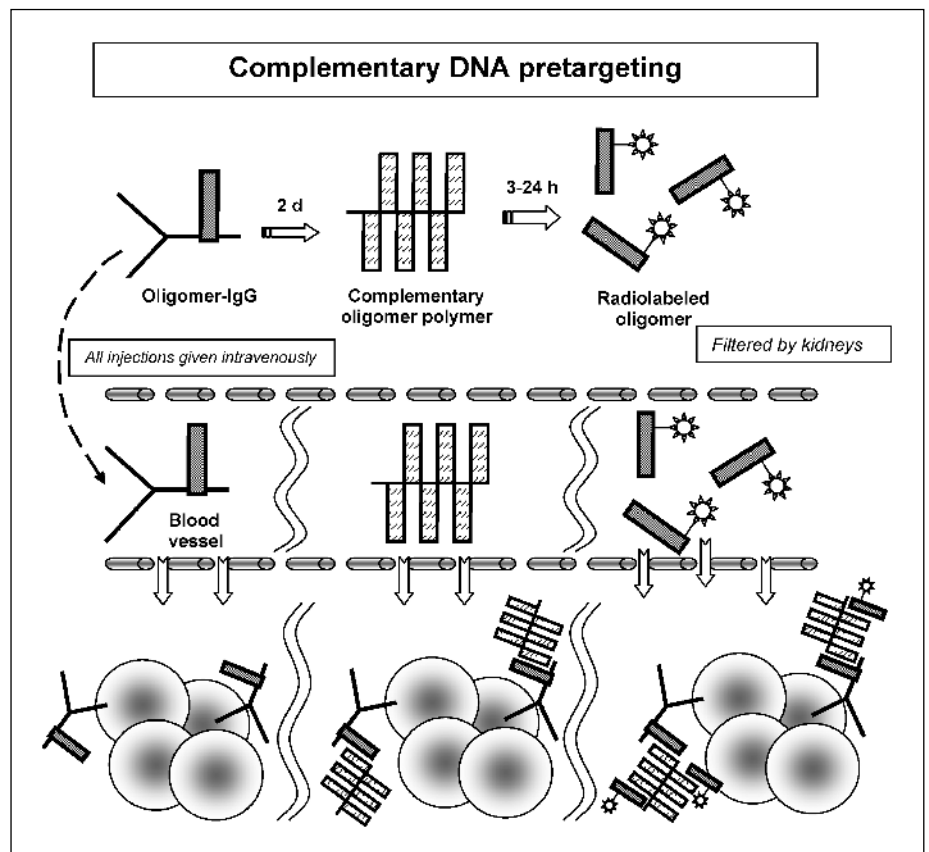


**Fig. 3.** Schematic representation of a pretargeting method that uses complementary oligonucleotides (morpholino compounds) as secondary recognition units. In this system, an oligo-conjugated IgG is given, and after suitable time for tumor localization and blood clearance, a complementary oligo is given, which is followed by the injection of the radiolabeled oligo.

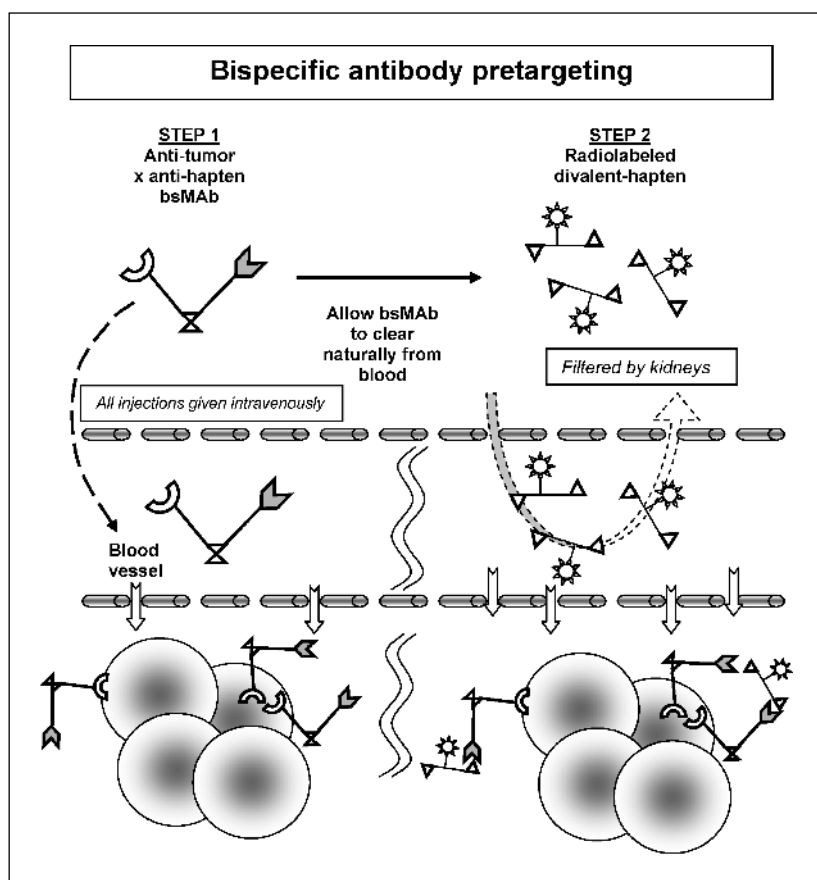


Fig. 4. The bispecific mAb pretargeting method. In the bispecific mAb/peptide-hapten pretargeting approach, a bispecific mAb, which has specificity to both a tumor antigen and the hapten, is given. Because most bispecific mAbs are small in size, after several days they have localized in the tumor and cleared from the blood sufficiently to allow for the radiolabeled hapten-peptide to be administered.

rapid clearance from the blood (46, 47). Nearly 15 years later, the first Food and Drug Administration–approved antibody-based, imaging agent was an  $^{111}\text{In}$ -labeled IgG for colorectal and ovarian cancer (48). Hepatic uptake of this agent hindered interpretation of possible metastases in the liver, but a  $^{99\text{m}}\text{Tc}$ -labeled anti–carcinoembryonic antigen (CEA) Fab' fragment improved the visualization of tumors in the liver (49). Currently,  $^{18}\text{F}$ deoxyglucose, with the improved sensitivity afforded by positron emission tomography imaging systems, has become the standard for oncology radionuclide imaging. However, there are several situations where interpretation based on  $^{18}\text{F}$ deoxyglucose positron emission tomography can be difficult due to its lack of specificity (50); therefore, the enhanced specificity afforded by an antibody-based imaging method would be important. Recent studies in animals bearing human colon tumor xenografts using a  $^{99\text{m}}\text{Tc}$ -labeled peptide in conjunction with a recombinant anti-CEA  $\times$  anti-HSG bispecific mAb have suggested that pretargeting methods can improve visualization of tumors so substantially compared with a directly radiolabeled F(ab') that this type of method could produce such superior images that it may be possible to use a standard gamma imaging system (51). Figure 5 shows the comparison of images seen with a pretargeting method versus a  $^{99\text{m}}\text{Tc}$ -anti-CEA Fab' at 1 and 24 hours, illustrating the superior visualization of tumor with the pretargeting method at each time. In fact, dynamic imaging studies (i.e., 2-minute images taken over the first 60 minutes after injection) have shown uptake in the tumor exceeding the heart within 20

minutes and exceeding the kidneys within 40 minutes (51). Tumor uptake of the radiolabeled peptide-hapten in this model can exceed that seen with the  $^{99\text{m}}\text{Tc}$ -Fab' by as much as 20-fold, providing superior signal strength in addition to more rapid and enhanced tumor/nontumor ratios. With the potential for specific delivery of the radiolabeled peptide-hapten within 1 hour, pretargeting methods could be adapted for use with many short-lived, positron-emitting radionuclides (52, 53), providing high sensitivity with greater specificity in situations where ambiguities related to the  $^{18}\text{F}$ deoxyglucose uptake are encountered.

### Pretargeting for Improved Therapy

Early studies clearly support the view that pretargeting increased tumor/nontumor ratios compared with direct targeting with a radiolabeled IgG, providing evidence that pretargeting would improve the therapeutic window of targeted radionuclides. However, because the radiolabeled compounds used in pretargeting cleared so rapidly from the blood, even with a larger therapeutic window, would it be possible for pretargeting to deliver a critical amount of radioactivity to the tumor to be therapeutic? Studies with directly radiolabeled antibodies have shown that as the molecular weight of the antibody decreases [e.g., from IgG to F(ab')<sub>2</sub> to Fab'], blood clearance is accelerated and the %ID/g delivered to the tumor decreases (54, 55). Because the radiolabeled compounds used in pretargeting were more than a log-fold smaller than the smallest antibody fragment tested with much faster clearance

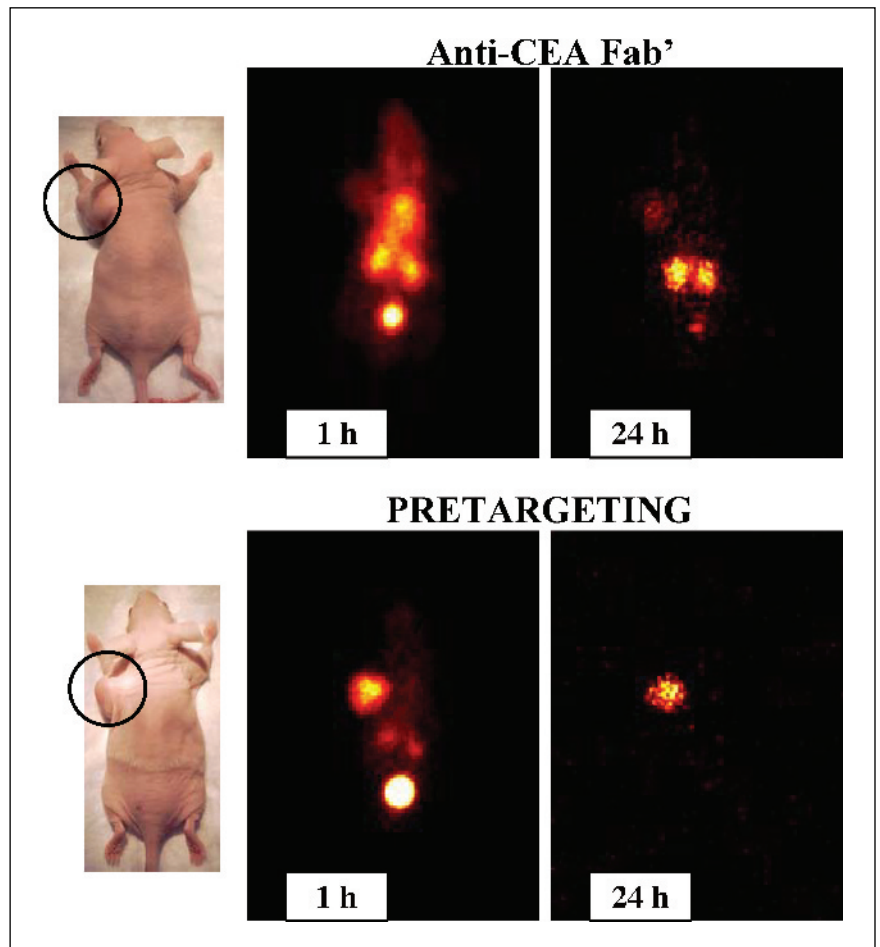
from the blood, it was likely that a substantially lower fraction of the administered radioactivity would be targeted to the tumor. Several of the early studies with bispecific mAb pretargeting reported uptake in the range 3% to 5% ID/g (56), but Axworthy et al. (57), using a "two-step" streptavidin-pretargeting method, showed that, when properly adjusted, the uptake of radiolabeled biotin was similar to that of the directly radiolabeled IgG and that this procedure could result in improved therapeutic responses compared with a directly radiolabeled IgG (58). Since then, there have been several other reports where the therapeutic efficacy of pretargeting is superior to direct targeting (59–63). We are finding similar experiences using a  $^{90}\text{Y}$ -DOTA-peptide-di-HSG hapten pretargeted by an anti-CEA  $\times$  anti-HSG bispecific mAb in a human colonic cancer xenograft model and in non-Hodgkin's lymphoma using chemically conjugated bispecific mAb composed of a humanized anti-CD20 Fab' (64) coupled to the murine anti-HSG Fab'.

The basis for pretargeting's ability to improve therapy is illustrated in Fig. 6 and Table 1. Figure 6 compares biodistribution data derived in nude mice bearing 0.4 to 1.0 g GW-39 human colonic tumors that were given  $^{111}\text{In}$ -DOTA anti-CEA IgG (hMN-14) or  $^{111}\text{In}$ -IMP-241, a di-HSG-DOTA peptide used in conjunction with a recombinant anti-CEA  $\times$  anti-HSG bispecific mAb. The recombinant bispecific mAb was given in a 10-fold mole excess of the moles of peptide injected, and a period of 24 hours was given before the injection of the  $^{111}\text{In}$ -IMP-241 to allow the bispecific mAb to clear from the blood

to  $<1.0\%$ ID/g. Fig. 6 (top) shows the biological uptake data expressed in %ID/g, whereas Fig. 6 (bottom) shows the effective clearance curves derived from these data. The effective curves are adjusted to show the amount of  $^{90}\text{Y}$  in the tumor, blood, and kidneys in nude mice at activity levels administered in the therapy study shown in Fig. 7 (i.e., 1.0 mCi  $^{90}\text{Y}$ -peptide-hapten versus 0.25 mCi  $^{90}\text{Y}$ -DOTA-IgG).

The biological clearance curves for  $^{90}\text{Y}$ -anti-CEA IgG show a tumor uptake of  $20.5 \pm 4.1\%$ ID/g at 24 hours, which remained relatively constant over 7 days. In contrast, the biological data for the pretargeting procedure show that tumor uptake was the highest at 3 hours, with  $21.4 \pm 3.7\%$ ID/g in the tumor and a steady decline over time. The loss of  $^{111}\text{In}$ -peptide-hapten from the tumor was related to the clearance of the bispecific mAb from the tumor (data not shown). Appreciable differences exist between the amount of radiolabeled IgG in the blood for the two procedures, with IgG at  $>30\%$ ID/g at 3 hours compared with  $\sim 2\%$  for the radiolabeled peptide-hapten in the pretargeting procedure. Under these conditions, tumor/blood ratios barely exceed 1:1 for the IgG by 24 hours, whereas, in pretargeting, the ratios are  $\sim 10:1$  at 3 hours. The effective clearance curves (bottom) clearly show that when administering equal toxic amounts of radioactivity, more radioactivity can be delivered to the tumor by the pretargeting method than by the directly radiolabeled IgG. Table 1 provides quantitative data from the effective clearance curves in terms of the area under the curve (AUC) and the average  $\mu\text{Ci/g}$  in the tumor and tissue

**Fig. 5.** Static images taken of nude mice bearing  $\sim 1.0$  g GW-39 human colonic tumor xenografts (top left shoulder, circled) and given either  $40 \mu\text{Ci } ^{99\text{m}}\text{Tc}$ -anti-CEA F(ab') (top) or  $40 \mu\text{Ci } ^{99\text{m}}\text{Tc}$ -peptide-di-HSG hapten 48 hours after the administration of a recombinant anti-CEA  $\times$  anti-HSG bispecific mAb (bottom). Anesthetized animals were placed face down on a low-energy, high-resolution collimator fitted to an ADAC Solus camera. The same animal in each group was imaged at 1 hour (100,000 counts per image) and 24 hours (20-minute images,  $\sim 12,000$ -15,000 counts per image) after the  $^{99\text{m}}\text{Tc}$  injections.



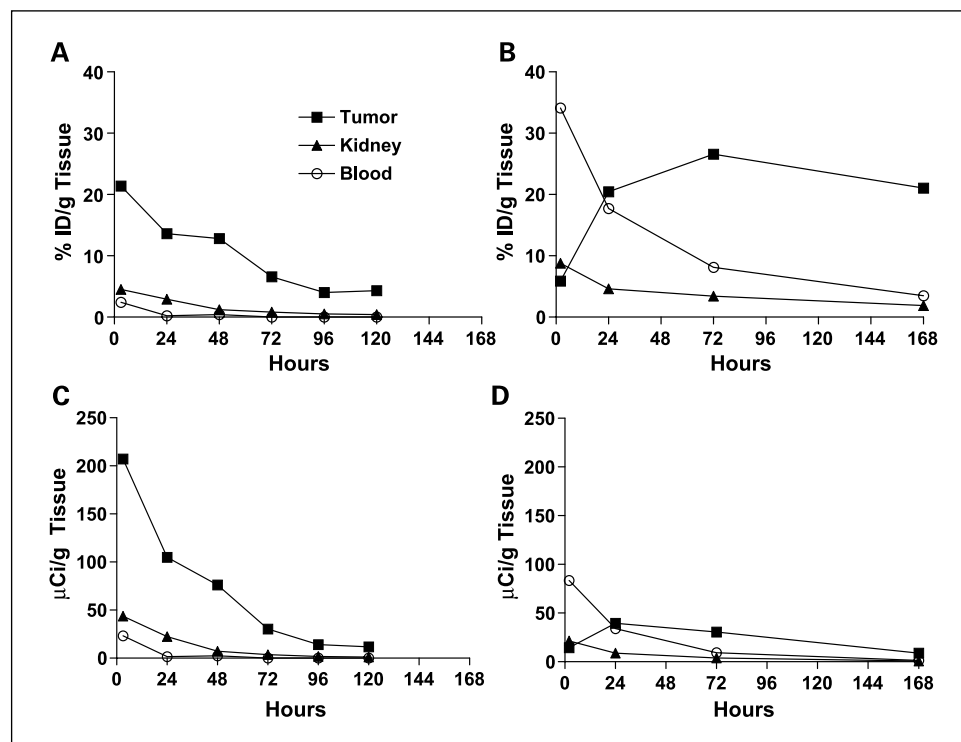


**Fig. 6.** Comparison of biological (top; %ID/g) and effective (bottom;  $\mu\text{Ci/g}$ ) uptake and clearance curves derived from i.v. injected  $^{111}\text{In}$ -DOTA-hMN-14 anti-CEA IgG (directly radiolabeled IgG; B and D) or  $^{111}\text{In}$ -IMP-241 peptide-hapten given 24 hours after the injection of an anti-CEA  $\times$  anti-HSG recombinant bispecific mAb (pretargeting; A and C). The biological curves represent the mean values taken from groups of five nude mice bearing 0.4 to 1.0 g s.c. GW-39 human colonic tumor xenografts. These data were then converted to  $\mu\text{Ci/g}$  by taking into account the physical decay of  $^{90}\text{Y}$  and then scaled to amount of  $^{90}\text{Y}$  radioactivity given to the mice in the therapy study shown in Fig. 7 (i.e., 1.0 mCi of the pretargeted  $^{90}\text{Y}$ -IMP-241 or 0.25 mCi  $^{90}\text{Y}$ -hMN-14 IgG). The AUC represents the integration of the time-activity curves to infinity from the curve-fit data.

over a 72-hour period for each procedure (the former value can be equated to total radiation dose, whereas the latter value can be equated to a radiation dose rate). The tumor AUC in the pretargeted animals is nearly twice the amount seen with the  $^{90}\text{Y}$ -IgG; therefore, a greater total radiation-absorbed dose would be delivered to the tumor. The tumor/blood AUC ratio for pretargeting was 22.6 compared with 1.6 for  $^{90}\text{Y}$ -IgG, also with a substantially lower average amount of radioactivity in the blood. Interestingly, the tumor/kidney ratio for the pretargeting procedure was 6:1 compared with 5:1 for the IgG, but in this case the average amount of radioactivity in the kidneys is  $\sim 1.5$ -fold higher than with the  $^{90}\text{Y}$ -IgG because of the higher amount of radioactivity administered.

The average amount of radioactivity ( $\mu\text{Ci/g}$ ) in the tumor and kidneys over the first 3 days would be  $\sim 1.5$  to 3 times higher with the pretargeting procedure compared with the  $^{90}\text{Y}$ -IgG, whereas the average  $\mu\text{Ci/g}$  to the blood (red marrow) would be  $\sim 5$  times higher with the  $^{90}\text{Y}$ -IgG. The determination of the average radioactivity in the tumor was truncated to 72 hours for all values primarily because 99% of the AUC for the blood in

the pretargeted animals was derived over this period of time, with 83% and 91% of the total AUC for the tumor and kidneys, respectively. For the IgG, 70% to 80% of the normal tissue AUC were derived within 72 hours, but only 47% of the total tumor AUC was derived over this time. Although a substantial portion of the total tumor AUC is derived after 72 hours, the average  $\mu\text{Ci/g}$  tumor is steadily declining. Thus, in this model, the projected radiation dose rate would be substantially lower, but was sustained for a longer period of time in the  $^{90}\text{Y}$ -IgG-treated animals than in the pretargeting setting. Although the specific extent to which a higher dose rate (i.e., average  $\mu\text{Ci/g}$  over time) would improve therapy is unknown, we suspect that it would have a positive influence on the therapeutic outcome.

Table 2 shows tumor uptake data derived from three animals that were used in a therapy study (Fig. 7). These animals, bearing GW-39 human colonic tumors that average  $0.475\text{ cm}^3$ , were injected with 0.25 mCi  $^{90}\text{Y}$ -hMN-14 anti-CEA IgG or with a recombinant anti-CEA  $\times$  anti-HSG bispecific mAb followed 1 day later with 1.0 mCi  $^{90}\text{Y}$ -IMP-241 peptide-hapten. One day after the  $^{90}\text{Y}$  injection, the animals were necropsied and

**Table 1.** Calculation of AUC and average  $\mu\text{Ci/g}$  in tumors over 72 hours for the bispecific mAb pretargeting procedure and directly radiolabeled IgG data shown in Fig. 3, modeling for  $^{90}\text{Y}$

Targeting method	Tumor		Kidneys		Blood	
	AUC ( $\mu\text{Ci h/g}$ )	$\mu\text{Ci/g}$ (72 h)	AUC ( $\mu\text{Ci h/g}$ )	$\mu\text{Ci/g}$ (72 h)	AUC ( $\mu\text{Ci h/g}$ )	$\mu\text{Ci/g}$ (72 h)
Pretargeting $^{90}\text{Y}$ -IMP-241 (1.0 mCi)	8,472	97.7	1,383	17.4	375	5.2
$^{90}\text{Y}$ -hMN-14 IgG (0.25 mCi)	4,801	31.7	932	9.2	3,005	28.2

NOTE: The average  $\mu\text{Ci/g}$  was calculated over 72 hours, because there was insufficient radioactivity left in the blood of the pretargeted animals to accurately assess the remaining activity; therefore, all values were truncated at this time.



**Table 2.** Dose calibrator readings from tumors taken 1 day after treatment with <sup>90</sup>Y-labeled product

Treatment (administered activity)	Total $\mu$ Ci		
	An 1	An 2	An 3
<sup>90</sup> Y-peptide pretargeting (1.0 mCi)	111.2	161.3	125.2
<sup>90</sup> Y-DOTA-IgG (0.25 mCi)	49.3	38.0	29.4

the tumors were read in a dose calibrator. On average, the pretargeting animals contained ~3.5-fold more <sup>90</sup>Y than the <sup>90</sup>Y-IgG animals, a finding that is consistent with the amount of radioactivity predicted in the tumors for each procedure by the effective clearance curves shown in Fig. 6 at 24 hours. Tumor growth was monitored in 10 animals for each treatment over a period of 14 weeks. Animals were removed from the study before this time if the tumor progressed to >2.5 cm<sup>3</sup> or became ulcerated, or if they had  $\geq$ 20% loss in body weight. Tumors in untreated animals progressed to >2.5 cm<sup>3</sup> within 2 weeks from the onset of the study (data not shown). With respect to the safety of these treatment doses, all but one animal survived the 1.0 mCi pretargeting treatment with an average of ~10% loss in body weight recorded 1 week after treatment as well as recovery within the next 2 weeks. One animal was found dead during week 11. This animal had recovered completely from an initial loss of 9% of body weight in first week but, by week 4, began to lose weight again. Before death, the animal's weight was stable for 5 weeks but at a level that was 10% to 13% lower than the starting weight. In the <sup>90</sup>Y-IgG group, two animals had to be removed from study within 4 weeks due to excessive weight loss, indicating the maximum tolerated dose had been exceeded at the 0.25 mCi dose of <sup>90</sup>Y-IgG. Another animal was removed from this group at week 10 because of an unexplained loss in body weight starting in the eighth week. Thus, although the 1.0 mCi pretargeted <sup>90</sup>Y-peptide dose seemed to be safely tolerated from a hematologic toxicity perspective (i.e., all animals survived over a 4- to 6-week period), because the effects of renal toxicity may occur months after treatment, additional studies assessing doses of 0.5 to 1.0 mCi of pretargeted <sup>90</sup>Y-peptide are currently under way to further assess safety over a period of 6 to 9 months. However, because of early deaths in the <sup>90</sup>Y-IgG-treated animals, lower doses must be used in future testing.

Irrespective of the treatment given, nearly all tumors experienced a doubling, or even quadrupling, in their mass over the first 2 to 4 weeks, at which time growth arrest occurred. Two animals had tumor progression or ulceration in the pretargeting group within the first 2 weeks, but at 14 weeks 7 of 10 animals in the pretargeting group had tumors <2.5 cm<sup>3</sup>. One of these seven tumors had evidence of progression starting in week 12 (i.e., 68% increase in tumor size from week 11 to 14), whereas the six others were stable throughout the observation period starting at 2 to 3 weeks after treatment. At the end of the study, only two animals in the <sup>90</sup>Y-IgG group remained with tumors  $\leq$ 2.5 cm<sup>3</sup>. Histologic examination of serial 5  $\mu$ m sections through the masses taken from the <sup>90</sup>Y-IgG group at the end of the study revealed no evidence of disease (cure) in one animal, with the other having 30% (the one showing progression) viable tumor. Histologic examination of the seven

tumor masses taken from the pretargeting group revealed that three were completely devoid of viable tumor. Thus, this single pretargeting treatment, which was safely tolerated in all animals, resulted in a 30% cure rate of substantially sized colonic tumors. Two of the other four tumors had only a single microscopic focus of viable cells, and the other two

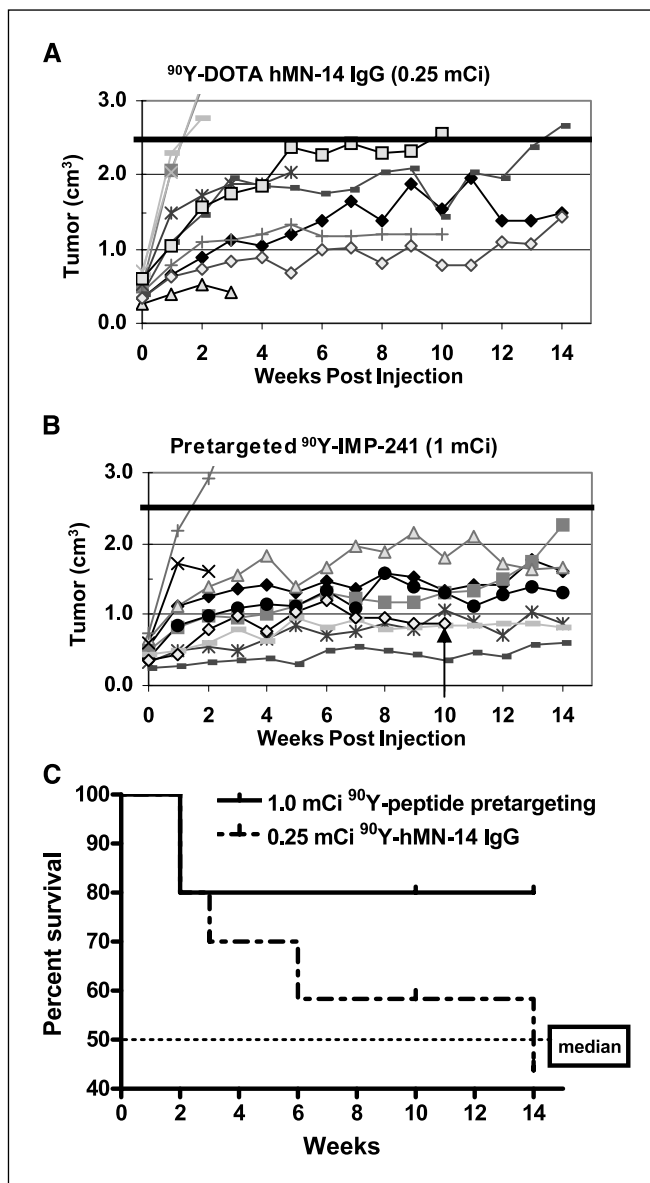


**Fig. 7.** Nude mice, averaging ~22 g in weight and bearing ~0.48 cm<sup>3</sup> s.c. GW-39 human tumor xenografts, were given either 1.0 mCi <sup>90</sup>Y-DOTA-peptide-di-HSG hapten 24 hours after receiving a recombinant anti-CEA  $\times$  anti-HSG bispecific mAb (10:1 bispecific mAb/peptide mole ratio) or 0.25 mCi <sup>90</sup>Y-DOTA-anti-CEA IgG. Growth curves for the individual animals given the <sup>90</sup>Y-anti-CEA IgG or the pretargeted <sup>90</sup>Y-DOTA-di-HSG peptide are shown in (A and B), respectively. The survival curves generated from these data using the time to progression to 2.5 cm<sup>3</sup> as the end point are shown in (C). Body weights and tumor size were measured weekly over a period of 14 weeks. Tumors in untreated animals of similar starting size progressed to >2.5 cm<sup>3</sup> within 2 to 3 weeks of the initiation of this study (data not shown). One animal in each group was removed because of a skin ulceration overlying the tumor. In the pretargeting group, this occurred 3 weeks after treatment in an animal with a starting tumor of 0.58 cm<sup>3</sup> that grew within 1 week to 1.7 cm<sup>3</sup>. In the <sup>90</sup>Y-IgG group, this occurred in an animal where the tumor had progressed to 2.0 cm<sup>3</sup> by week 5. One animal in the pretargeting group was found dead at the start of week 11 (arrow in B), whereas three animals were removed due to  $\geq$ 20% loss in body weight in the <sup>90</sup>Y-IgG group (two at week 3 and one at week 10).

Downloaded from http://aacrjournals.org/clinccancerres/article-pdf/11/19/7109s/1920907/7109s-711s.pdf by guest on 10 August 2024

tumors were composed of ~30% to 70% (the latter one having evidence of progression) viable tumor cells. These preliminary results are highly encouraging and support the superiority of the pretargeting treatment in this human colonic cancer model.

Pretargeting systems have also been tested clinically in solid tumors. Using the same two-step streptavidin pretargeting approach with the NR-LU-10 antibody and  $^{90}\text{Y}$ -biotin as tested preclinically by Axworthy et al. (58), investigators found excellent targeting of tumor lesions, but unfortunately the specificity of the NR-LU-10 antibody for the gastrointestinal tract also resulted in excellent targeting of this organ, which in turn caused dose-limiting gastrointestinal toxicity in therapy trials (65–67). In addition, at the highest doses of  $^{90}\text{Y}$ -biotin tested, renal toxicity was encountered in a few patients, occurring several months after treatment (66, 67). The potential for renal toxicity could have been predicted from animal studies, which showed pretargeting procedures to be so highly efficient at removing radioactivity from the blood that the total injected activity could be increased substantially compared with a directly radiolabeled IgG. The vast majority of the injected activity is quickly eliminated by urinary excretion (e.g., ~80% within a few hours); therefore, the kidneys are exposed to higher levels of radioactivity during this rapid transport process. In our experience, the radiolabeled peptide-hapten compounds typically have a maximum of only ~3% to 5% ID/g in the kidneys of mice within the first 3 hours, which decreases slowly over time. This uptake is 10 to 20 times lower than that seen with an antibody fragment radiolabeled directly with a radiometal (68) and in many cases is actually lower than that found in the kidneys with a directly radiolabeled IgG (42, 45, 54, 55). However, because considerably more radioactivity is injected with a pretargeted radionuclide therapeutic procedure than a directly radiolabeled IgG (in our preclinical experience, ~4- to 5-fold higher), the total amount of radioactivity passing through and subsequently localizing in the kidneys is higher. Nevertheless, renal excretion of the radiolabeled compound is preferred over hepatobiliary/intestinal excretion because of the higher radiation sensitivity of the gastrointestinal tract. Thus, although pretargeting procedures significantly reduce red marrow exposure, there is an increased risk for renal damage; therefore, investigators need to carefully monitor short-term and long-term effects to the kidneys. However, as shown in animals by Subbiah et al. (59), severe hematologic toxicity does occur in pretargeting, which could result in dose-limiting toxicity. This is not surprising, given the radiosensitivity differences between the bone marrow and kidneys. Subbiah et al. (59) also examined serum biochemistries for evidence of renal toxicity, but this examination only spanned 28 days, a period that is likely too short to detect changes in renal function. Indeed, others have reported renal toxicity by serum chemistries and histologic examination of the kidneys in mice several months after treatment (69, 70), which is similar to the clinical experience with pretargeting procedures using  $^{90}\text{Y}$ -biotin (66, 67) or even with a  $^{90}\text{Y}$ -labeled peptide (71).

A phase II trial was done in colorectal cancer using a dose of 110 mCi/m<sup>2</sup> of the  $^{90}\text{Y}$ -biotin (67). Gastrointestinal-related toxicities were the major side effect, but even at this dose two patients developed significant elevations (grades 3 and 4) of serum creatinine 7 to 8 months after treatment. Grade 4

hematologic toxicities were found in six cases, but most patients only had grade  $\leq 2$ . Two of the 25 patients studied on this trial had partial responses lasting 16 weeks, and 4 patients had stable disease for 10 to 20 weeks. Clinical studies using the three-step streptavidin method have not reported similar toxicities, but this most likely reflects the application of this model predominantly in the intracompartmental treatment of brain or ovarian cancers using less radioactivity (72, 73). Phase I studies using a bispecific mAb pretargeting method and an  $^{131}\text{I}$ -labeled peptide-hapten have been reported in lung, colorectal, and medullary thyroid cancer patients, and interestingly, in all of these trials, dose escalation has been limited by hematologic toxicity (41, 74, 75). Some responses were observed in these trials, but overall it has been difficult to show responses in clinical trials of patients with solid tumors that are generally fairly radioresistant. However, a recent examination of patients with medullary thyroid cancer treated with the bispecific mAb pretargeting procedure suggests that, based on a reduction or stabilization of tumor markers and survival, clinical benefit may have occurred in those patients treated previously with a pretargeting procedure (76). In addition, this group has found evidence, at least in medullary thyroid cancer, that there may be bone marrow involvement that is not appreciated by standard examinations, which could explain the higher level of hematologic toxicity observed in these patients (41, 77).

Although pretargeting has been equally challenging for the treatment of most solid tumors, there are recent indications suggesting that pretargeting can improve the treatment of non-Hodgkin's lymphoma compared with directly radiolabeled IgG. Press et al. (62) have shown improved therapeutic responses with a two-step pretargeting procedure using a streptavidin-anti-CD20 conjugate and  $^{90}\text{Y}$ -biotin compared with the  $^{90}\text{Y}$ -anti-CD20 IgG. We are also exploring the potential for using a bispecific mAb pretargeting approach to improve radioimmunotherapy of non-Hodgkin's lymphoma in animals bearing Ramos tumor xenografts (78). In the study shown in Fig. 8, 10 BALB/c nude mice bearing  $0.57 \pm 0.11 \text{ cm}^3$  s.c. Ramos human B-cell tumors were given the anti-CD20 (hA20)  $\times$  anti-HSG bispecific mAb and 48 hours later received 0.8 mCi  $^{90}\text{Y}$ -DOTA-peptide-hapten. Another group of 10 animals bearing  $0.57 \pm 0.14 \text{ cm}^3$  tumors was given 0.175 mCi  $^{90}\text{Y}$ -DOTA humanized anti-CD20 IgG (same anti-CD20 antibody used to prepare the bispecific mAb). These radioactivity dose levels were believed to represent 80% of the maximum tolerated dose for the pretargeted and directly radiolabeled antibody treatments based on earlier observations in nude mice treated with the anti-CEA bispecific mAb pretargeting procedure and the same  $^{90}\text{Y}$ -DOTA-peptide-hapten or the  $^{90}\text{Y}$ -DOTA-anti-CEA IgG (see above). However, in this study, two animals in the  $^{90}\text{Y}$ -IgG group were removed due to excessive weight loss within 2 and 4 weeks of the onset of treatment. The animal removed at 4 weeks initially showed a good response to the treatment but had evidence of tumor progression when removed from the study. The other animal was removed too early to assess antitumor activity reliably. Two animals were also removed from the pretargeted group due to weight loss, but at 11 and 16 weeks after treatment. Importantly, both of these animals were tumor free at these times. The specific cause of the toxicity in all of these animals was not determined, but these animals were all ~4 g smaller than the animals used in

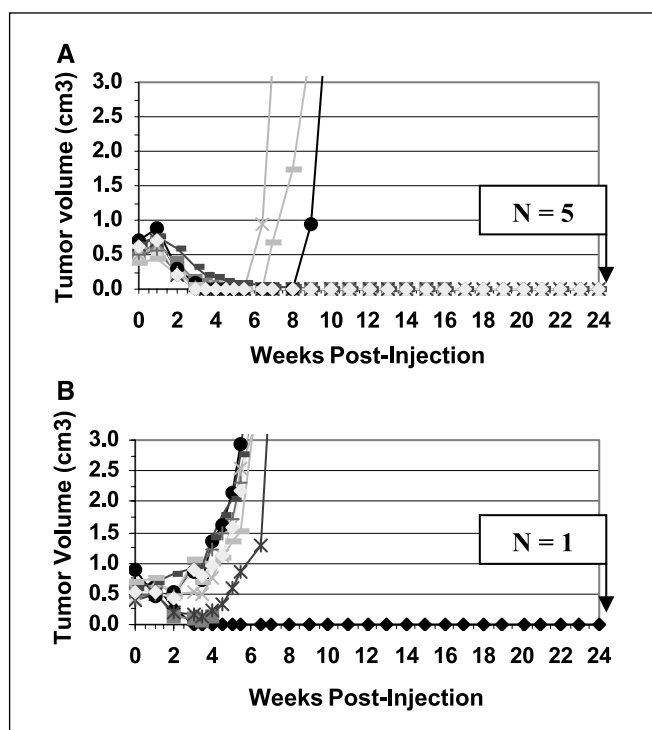


**Fig. 8.** Growth curves of s.c. Ramos human B-cell lymphoma xenografts in BALB/c nude mice (~18 g body weight) after treatment with either 0.8 mCi  $^{90}\text{Y}$ -DOTA-peptide-di-HSG hapten given 48 hours after an anti-CD20 F(ab') $\times$  anti-HSG F(ab') bispecific mAb (A) or 0.175 mCi  $^{90}\text{Y}$ -anti-CD20 IgG (B). Ten animals were in each treatment group. A separate group of untreated animals or animals given 0.8 mCi  $^{90}\text{Y}$ -DOTA-peptide-di-HSG hapten was included as controls, but their tumors progressed within 2 to 3 weeks of the onset of the study (data not shown). Body weights and tumor size were measured weekly for a period of 6 months. At the end of the study, only one animal remained tumor-free in the  $^{90}\text{Y}$ -anti-CD20 IgG group, whereas there were five tumor-free animals in the pretargeted-treated group.

previous studies; therefore, it is likely that they were not able to tolerate the same amount of  $^{90}\text{Y}$ -radioactivity used in the earlier studies.

Control animals (data not shown) given either 0.8 mCi  $^{90}\text{Y}$ -peptide-hapten alone or left untreated had tumor progression to  $>2.5\text{ cm}^3$  within 2 to 3 weeks. After 24 weeks of observation, only one of the eight surviving animals in the  $^{90}\text{Y}$ -IgG group was tumor free, with the other surviving animals removed between weeks 5 and 7 because of rapidly growing tumors. In contrast, in the pretargeting group, five of eight surviving animals remained tumor-free (cure) at the end of the study, again supporting the improved therapeutic efficacy for a pretargeting procedure compared with a directly radiolabeled antibody (Fig. 8).

Two pilot clinical studies have been done with the two-step streptavidin pretargeting procedure in patients with non-Hodgkin's lymphoma, one using a rituximab-streptavidin conjugate and the other a recombinant anti-CD20-streptavidin fusion protein, with both using  $^{90}\text{Y}$ -biotin as the therapeutic agent (79, 80). Doses of up to 50 mCi/m $^2$  were tolerated in the former study in a heavily pretreated patient population (79). The latter report focused primarily on the pharmacokinetics, targeting, and dosimetry of the system, but a dose of 15 mCi/m $^2$  of  $^{90}\text{Y}$ -biotin was given to 14 patients. In this study, the absorbed dose to the tumors averaged  $26 \pm 4$  cGy/mCi with a marrow dose of only 0.2 cGy/mCi. Kidney and bladder doses

were estimated to be  $\sim 7.0$  cGy/mCi. Although the average radiation-absorbed dose/mCi to the tumor was about half of that reported for  $^{90}\text{Y}$ -ibritumomab (anti-CD20 IgG; ref. 81), only 11 of 14 patients given  $^{90}\text{Y}$ -DOTA-biotin at a dose of 15 mCi/m $^2$ , which is similar to the maximum recommended dose of 0.4 mCi/kg  $^{90}\text{Y}$ -ibritumomab, had gradable hematologic toxicity, suggesting that substantially higher doses of the pretargeted  $^{90}\text{Y}$ -biotin would be possible, with the potential to increase the total radiation-absorbed dose delivered to tumors. In both trials, a substantial fraction of the patients developed an anti-streptavidin response, which would likely limit the treatment to a single course.

## Conclusions

The data summarized herein and in the literature support the view that pretargeting should be the preferred method for delivering radionuclides for imaging and therapeutic applications. Pretargeting methods can deliver more radioactivity to tumors than a directly radiolabeled antibody fragment, which improves the signal strength that is important for obtaining high counting statistics and less ambiguous images. Tumor/nontumor ratios for pretargeting methods are highly favorable for imaging within 1 hour, which would be useful for a wide range of positron-emitting radionuclides, although the excellent uptake and contrast ratios with pretargeting seen with a  $^{99\text{m}}\text{Tc}$ -peptide-hapten may be sufficient to allow for excellent sensitivity even with standard gamma imaging systems.

For therapy, there are several preclinical models showing the superiority of pretargeting to a directly radiolabeled antibody. Although improvement in radionuclide delivery and therapeutic responses has been observed in preclinical models, it remains to be determined whether pretargeting can bring about objective responses in patients with advanced solid tumors. In addition, there have been several clinical trials exploring the combination of radioimmunotherapy with directly radiolabeled antibodies and chemotherapy, where pretargeting might hold a key advantage over directly radiolabeled antibody, particularly if the chemotherapeutic agent is myelosuppressive. Animal studies have already shown that pretargeting can be effectively combined with chemotherapy to increase antitumor activity (82, 83). Although solid tumors will remain a challenge, preclinical and initial clinical studies suggest that pretargeting would likely be an advantage for use in non-Hodgkin's lymphoma over the currently approved radiolabeled antibodies.

Although pretargeting procedures have been considered in the past to be somewhat cumbersome, there has been a renewed and encouraging interest in this methodology. Thus, we believe that pretargeting procedures will represent not only the next generation for the specific and increased delivery of radionuclides for cancer imaging and therapy but also may provide improved delivery systems for other contrast agents for magnetic resonance imaging and ultrasound, and perhaps also for drugs in a variety of diseases.

## Acknowledgments

We thank Jessica Kearney, Dion Yeldell, Nino Velasco, and Guy Newsome for technical assistance.

References

1. Kelloff GJ, Hoffman JM, Johnson B, et al. Progress and promise of FDG-PET imaging for cancer patient management and oncologic drug development. *Clin Cancer Res* 2005;11:2785–808.
2. Larson SM, Krenning EP. A pragmatic perspective on molecular targeted radionuclide therapy. *J Nucl Med* 2005;46:1–35.
3. Goldenberg DM. Targeted therapy of cancer with radiolabeled antibodies. *J Nucl Med* 2002;43:693–713.
4. Goldenberg DM, Preston DF, Primus FJ, Hansen HJ. Photoscan localization of GW-39 tumors in hamsters using radiolabeled anticarcinoembryonic antigen immunoglobulin G. *Cancer Res* 1974;34:1–9.
5. Goldenberg DM, Deland F, Kim E, et al. Use of radiolabeled antibodies to carcinoembryonic antigen for the detection and localization of diverse cancers by external photoscanning. *N Engl J Med* 1978;298:1384–6.
6. Schlom J, Hand PH, Greiner JW, et al. Innovations that influence the pharmacology of monoclonal antibody guided tumor targeting. *Cancer Res* 1990;50:820–7s.
7. Sharkey RM, Boerman OC, Natale A, et al. Enhanced clearance of radiolabeled murine monoclonal antibody by a syngeneic anti-idiotypic antibody in tumor-bearing nude mice. *Int J Cancer* 1992;51:266–73.
8. DeNardo GL, Maddock SW, Sgouros G, Scheibe PO, DeNardo SJ. Immunoadsorption: an enhancement strategy for radioimmunotherapy. *J Nucl Med* 1993;34:1020–7.
9. Wang Z, Garkavij M, Ohlsson T, Strand SE, Sjogren HO, Tennvall J. Biotinylation, pharmacokinetics, and extracorporeal adsorption of humanized MAb <sup>111</sup>In-MN14 using an avidin-affinity column in rats. *Cancer Biother Radiopharm* 2003;18:365–75.
10. Sharkey RM, Motta-Hennessy C, Pawlyk D, Siegel JA, Goldenberg DM. Biodistribution and radiation dose estimates for yttrium- and iodine-labeled monoclonal antibody IgG and fragments in nude mice bearing human colonic tumor xenografts. *Cancer Res* 1990;50:2330–6.
11. Behr TM, Behe M, Stabin MG, et al. High-linear energy transfer (LET)  $\alpha$  versus low-LET  $\beta$  emitters in radioimmunotherapy of solid tumors: therapeutic efficacy and dose-limiting toxicity of <sup>213</sup>Bi- versus <sup>90</sup>Y-labeled CO17-1A Fab' fragments in a human colonic cancer model. *Cancer Res* 1999;59:2635–43.
12. Reardan DT, Meares CF, Goodwin DA, et al. Antibodies against metal chelates. *Nature* 1985;316:265–8.
13. Goodwin DA, Meares CF, David GF, et al. Monoclonal antibodies as reversible equilibrium carriers of radiopharmaceuticals. *Int J Rad Appl Instrum B* 1986;13:383–91.
14. Goodwin DA, Meares CF, McCall MJ, McTigue M, Chaovapong W. Pre-targeted immunoscintigraphy of murine tumors with indium-111-labeled bifunctional haptens. *J Nucl Med* 1988;29:226–34.
15. Stickney DR, Anderson LD, Slater JB, et al. Bifunctional antibody: a binary radiopharmaceutical delivery system for imaging colorectal carcinoma. *Cancer Res* 1991;51:6650–5.
16. Hnatowich DJ, Virzi F, Ruscowski M. Investigations of avidin and biotin for imaging applications. *J Nucl Med* 1987;28:1294–302.
17. Bagshawe KD, Sharma SK, Begent RH. Antibody-directed enzyme prodrug therapy (ADEPT) for cancer. *Expert Opin Biol Ther* 2004;4:1777–89.
18. McKeown SR, Ward C, Robson T. Gene-directed enzyme prodrug therapy: a current assessment. *Curr Opin Mol Ther* 2004;6:421–35.
19. Satchi R, Connors TA, Duncan R. PDEPT: polymer-directed enzyme prodrug therapy. I. HPMA copolymer-cathepsin B and PK1 as a model combination. *Br J Cancer* 2001;85:1070–6.
20. Park YJ, Liang JF, Song H, Li YT, Naik S, Yang VC. ATTEMPTS: a heparin/protamine-based triggered release system for the delivery of enzyme drugs without associated side-effects. *Adv Drug Deliv Rev* 2003;55:251–65.
21. Ong GL, Ettenson D, Sharkey RM, et al. Galactose-conjugated antibodies in cancer therapy: properties and principles of action. *Cancer Res* 1991;51:1619–26.
22. Jitrapakdee S, Wallace JC. The biotin enzyme family: conserved structural motifs and domain rearrangements. *Curr Protein Pept Sci* 2003;4:217–29.
23. Hnatowich DJ. The *in vivo* uses of streptavidin and biotin: a short progress report. *Nucl Med Commun* 1994;15:575–7.
24. Rosebrough SF, Hartley DF. Quantification and lowering of serum biotin. *Lab Anim Sci* 1995;45:554–7.
25. Kalofonos HP, Ruscowski M, Siebecker DA, et al. Imaging of tumor in patients with indium-111-labeled biotin and streptavidin-conjugated antibodies: preliminary communication. *J Nucl Med* 1990;31:1791–6.
26. Sharkey RM, Karacay H, Griffiths GL, et al. Development of a streptavidin-anti-carcinoembryonic antigen antibody, radiolabeled biotin pretargeting method for radioimmunotherapy of colorectal cancer. Studies in a human colon cancer xenograft model. *Bioconjug Chem* 1997;8:595–604.
27. Cremonesi M, Ferrari M, Chinol M, et al. Three-step radioimmunotherapy with yttrium-90 biotin: dosimetry and pharmacokinetics in cancer patients. *Eur J Nucl Med* 1999;26:110–20.
28. Paganelli G, Pervez S, Siccardi AG, et al. Intraperitoneal radio-localization of tumors pre-targeted by biotinylated monoclonal antibodies. *Int J Cancer* 1990;45:1184–9.
29. Liu G, Mangera K, Liu N, Gupta S, Ruscowski M, Hnatowich DJ. Tumor pretargeting in mice using <sup>99m</sup>Tc-labeled morpholino, a DNA analog. *J Nucl Med* 2002;43:384–91.
30. Liu G, Liu C, Zhang S, et al. Investigations of <sup>99m</sup>Tc morpholino pretargeting in mice. *Nucl Med Commun* 2003;24:697–705.
31. Liu G, He J, Dou S, et al. Pretargeting in tumored mice with radiolabeled morpholino oligomer showing low kidney uptake. *Eur J Nucl Med Mol Imaging* 2004;31:417–24.
32. He J, Liu G, Gupta S, Zhang Y, Ruscowski M, Hnatowich DJ. Amplification targeting: a modified pretargeting approach with potential for signal amplification-proof of a concept. *J Nucl Med* 2004;45:1087–95.
33. Feng X, Pak RH, Kroger LA, et al. New anti-Cu-TETA and anti-Y-DOTA monoclonal antibodies for potential use in the pre-targeted delivery of radiopharmaceuticals to tumor. *Hybridoma* 1998;17:125–32.
34. Goodwin DA, Meares CF, Watanabe N, et al. Pharmacokinetics of pretargeted monoclonal antibody 2D12.5 and <sup>88</sup>Y-Janus-2-(*p*-nitrobenzyl)-1,4,7,10-tetraazacyclododecanetetraacetic acid (DOTA) in BALB/c mice with KHJJ mouse adenocarcinoma: a model for <sup>90</sup>Y radioimmunotherapy. *Cancer Res* 1994;54:5937–46.
35. Le Doussal JM, Martin M, Gautherot E, Delaage M, Barbet J. *In vitro* and *in vivo* targeting of radiolabeled monovalent and divalent haptens with dual specificity monoclonal antibody conjugates: enhanced divalent hapten affinity for cell-bound antibody conjugate. *J Nucl Med* 1989;30:1358–66.
36. Boerman OC, Kranenborg MH, Oosterwijk E, et al. Pretargeting of renal cell carcinoma: improved tumor targeting with a bivalent chelate. *Cancer Res* 1999;59:4400–5.
37. Karacay H, McBride WJ, Griffiths GL, et al. Experimental pretargeting studies of cancer with a humanized anti-CEA  $\times$  murine anti-[In-DTPA] bispecific antibody construct and a <sup>99m</sup>Tc-/<sup>188</sup>Re-labeled peptide. *Bioconjug Chem* 2000;11:842–54.
38. Rossi EA, Sharkey RM, McBride W, et al. Development of new multivalent-bispecific agents for pretargeting tumor localization and therapy. *Clin Cancer Res* 2003;9:3886–96S.
39. Rossi EA, Chang C-H, Losman MJ, et al. Pretargeting of CEA-expressing cancers with a trivalent bispecific fusion protein produced in myeloma cells. *Clin Cancer Res (Suppl)* 2005;11:7122s–9s.
40. Sharkey RM, Karacay H, Richel H, et al. Optimizing bispecific antibody pretargeting for use in radioimmunotherapy. *Clin Cancer Res* 2003;9:3897–913S.
41. Kraeber-Bodere F, Faivre-Chauvet A, Ferrer L, et al. Pharmacokinetics and dosimetry studies for optimization of anti-carcinoembryonic antigen  $\times$  anti-hapten bispecific antibody-mediated pretargeting of iodine-131-labeled hapten in a phase I radioimmunotherapy trial. *Clin Cancer Res* 2003;9:3973–81S.
42. Sharkey RM, McBride WJ, Karacay H, et al. A universal pretargeting system for cancer detection and therapy using bispecific antibody. *Cancer Res* 2003;63:354–63.
43. Janevik-Ivanovska E, Gautherot E, Hillairet de Boisferon M, et al. Bivalent hapten-bearing peptides designed for iodine-131 pretargeted radioimmunotherapy. *Bioconjug Chem* 1997;8:526–33.
44. Goodwin DA, Meares CF, McTigue M, et al. Pretargeted immunoscintigraphy: effect of hapten valency on murine tumor uptake. *J Nucl Med* 1992;33:2006–13.
45. Karacay H, Sharkey RM, McBride WJ, et al. Pretargeting for cancer radioimmunotherapy with bispecific antibodies: role of the bispecific antibody's valency for the tumor target antigen. *Bioconjug Chem* 2002;13:1054–70.
46. Mach JP, Forni M, Ritschard J, et al. Use of limitations of radiolabeled anti-CEA antibodies and their fragments for photoscanning detection of human colorectal carcinomas. *Oncodev Biol Med* 1980;1:49–69.
47. Wahl RL, Parker CW, Philpott GW. Improved radioimaging and tumor localization with monoclonal F(ab)<sub>2</sub>. *J Nucl Med* 1983;24:316–25.
48. Nabi HA, Doerr RJ. Radiolabeled monoclonal antibody imaging (immunoscintigraphy) of colorectal cancers: current status and future perspectives. *Am J Surg* 1992;163:448–56.
49. Moffat FL, Jr., Pinsky CM, Hammershaimb L, et al. Clinical utility of external immunoscintigraphy with the IMMU-4 technetium-99 m Fab' antibody fragment in patients undergoing surgery for carcinoma of the colon and rectum: results of a pivotal, phase III trial. The Immunomedics Study Group. *J Clin Oncol* 1996;14:2295–305.
50. Rohren EM, Turkington TG, Coleman RE. Clinical applications of PET in oncology. *Radiology* 2004;231:305–32.
51. Sharkey RM, Cardillo TM, Rossi EA, et al. Signal amplification in molecular imaging by pretargeting a multivalent bispecific nanobody. *Nat Med*. In press 2005.
52. Griffiths GL, Chang CH, McBride WJ, et al. Reagents and methods for PET using bispecific antibody pretargeting and <sup>68</sup>Ga-radiolabeled bivalent hapten-peptide-chelate conjugates. *J Nucl Med* 2004;45:30–9.
53. Schuhmacher J, Kaul S, Klivenyi G, et al. Immunoscintigraphy with positron emission tomography: gallium-68 chelate imaging of breast cancer pretargeted with bispecific anti-MUC1/anti-Ga chelate antibodies. *Cancer Res* 2001;61:3712–7.
54. Sharkey RM, Motta-Hennessy C, Pawlyk D, Siegel JA, Goldenberg DM. Biodistribution and radiation dose estimates for yttrium- and iodine-labeled monoclonal antibody IgG and fragments in nude mice bearing human colonic tumor xenografts. *Cancer Res* 1990;50:2330–6.
55. Sharkey RM, Blumenthal RD, Hansen HJ, Goldenberg DM. Biological considerations for radioimmunotherapy. *Cancer Res* 1990;50:964–9s.
56. Boerman OC, van Schaik FG, Oyen WJ, Corstens FH. Pretargeted radioimmunotherapy of cancer: progress step by step. *J Nucl Med* 2003;44:400–11.
57. Axworthy DB, Fritzberg AR, Hylarides MD, et al. Preclinical evaluation of an anti-tumor monoclonal antibody/streptavidin conjugate for pretargeted <sup>90</sup>Y radioimmunotherapy in a mouse xenograft model [abstract]. *J Immunother* 1994;16:158.
58. Axworthy DB, Reno JM, Hylarides MD, et al. Cure of human carcinoma xenografts by a single dose of

Downloaded from <http://aacrjournals.org/clinccancerres/article-pdf/11/19/7122s/19209077/109s-7121s.pdf> by guest on 10 August 2024

- pretargeted yttrium-90 with negligible toxicity. *Proc Natl Acad Sci U S A* 2000;97:1802–7.
59. Subbiah K, Hamlin DK, Pagel JM, et al. Comparison of immunoscintigraphy, efficacy, and toxicity of conventional and pretargeted radioimmunotherapy in CD20-expressing human lymphoma xenografts. *J Nucl Med* 2003;44:437–45.
60. Gautherot E, Rouvier E, Daniel L, et al. Pretargeted radioimmunotherapy of human colorectal xenografts with bispecific antibody and <sup>131</sup>I-labeled bivalent hapten. *J Nucl Med* 2000;41:480–7.
61. Kraeber-Bodere F, Faibre-Chauvet A, Sai-Maurel C, et al. Bispecific antibody and bivalent hapten radioimmunotherapy in CEA-producing medullary thyroid cancer xenograft. *J Nucl Med* 1999;40:198–204.
62. Press OW, Corcoran M, Subbiah K, et al. A comparative evaluation of conventional and pretargeted radioimmunotherapy of CD20-expressing lymphoma xenografts. *Blood* 2001;98:2535–43.
63. Zhang M, Zhang Z, Garmestani K, et al. Pretarget radiotherapy with an anti-CD25 antibody-streptavidin fusion protein was effective in therapy of leukemia/lymphoma xenografts. *Proc Natl Acad Sci U S A* 2003;100:1891–5.
64. Stein R, Qu Z, Chen S, et al. Characterization of a new humanized anti-CD20 monoclonal antibody, IMM106, and its use in combination with the humanized anti-CD22 antibody, epratuzumab, for the therapy of non-Hodgkin's lymphoma. *Clin Cancer Res* 2004;10:2868–78.
65. Breitz HB, Weiden PL, Beaumier PL, et al. Clinical optimization of pretargeted radioimmunotherapy with antibody-streptavidin conjugate and <sup>90</sup>Y-DOTA-biotin. *J Nucl Med* 2000;41:131–40.
66. Breitz HB, Fisher DR, Goris ML, et al. Radiation absorbed dose estimation for <sup>90</sup>Y-DOTA-biotin with pretargeted NR-LU-10/streptavidin. *Cancer Biother Radiopharm* 1999;14:381–95.
67. Knox SJ, Goris ML, Tempero M, et al. Phase II trial of yttrium-90-DOTA-biotin pretargeted by NR-LU-10 antibody/streptavidin in patients with metastatic colon cancer. *Clin Cancer Res* 2000;6:406–14.
68. Behr TM, Sharkey RM, Juweid ME, et al. Reduction of the renal uptake of radiolabeled monoclonal antibody fragments by cationic amino acids and their derivatives. *Cancer Res* 1995;55:3825–34.
69. Adams GP, Shaller CC, Dadachova E, et al. A single treatment of yttrium-90-labeled CHX-A<sup>2</sup>C6.5 diabody inhibits the growth of established human tumor xenografts in immunodeficient mice. *Cancer Res* 2004;64:6200–6.
70. Furmanova P, Challer C, Simmons H, Adams G. An evaluation of the damage to the normal tissues resulting from radioimmunotherapy with anti-HER2 diabodies [abstract]. *Cancer Biother Radiopharm* 2004;19:517.
71. Paganelli G, Zoboli S, Cremonesi M, et al. Receptor-mediated radiotherapy with <sup>90</sup>Y-DOTA-D-Phe1-Tyr3-octreotide. *Eur J Nucl Med* 2001;28:426–34.
72. Grana C, Bartolomei M, Handkiewicz D, et al. Radioimmunotherapy in advanced ovarian cancer: is there a role for pre-targeting with <sup>90</sup>Y-biotin? *Gynecol Oncol* 2004;93:691–8.
73. Paganelli G, Bartolomei M, Ferrari M, et al. Pretargeted locoregional radioimmunotherapy with <sup>90</sup>Y-biotin in glioma patients: phase I study and preliminary therapeutic results. *Cancer Biother Radiopharm* 2001;16:227–35.
74. Vuillez JP, Kraeber-Bodere F, Moro D, et al. Radioimmunotherapy of small cell lung carcinoma with the two-step method using a bispecific anti-carcinoembryonic antigen/anti-diethylenetriaminepentaacetic acid (DTPA) antibody and iodine-131 di-DTPA hapten: results of a phase I/II trial. *Clin Cancer Res* 1999;5:3259–67s.
75. Kraeber-Bodere F, Bardet S, Hoefnagel CA, et al. Radioimmunotherapy in medullary thyroid cancer using bispecific antibody and iodine 131-labeled bivalent hapten: preliminary results of a phase I/II clinical trial. *Clin Cancer Res* 1999;5:3190–8s.
76. Barbet J, Kraeber-Bodere F, Champion L, Chatal JF. Results of a pretargeted radioimmunotherapy (RIT) phase I/II trial in medullary thyroid carcinoma (MTC): biological markers and effects on survival [abstract]. *Cancer Biother Radiopharm* 2004;19:523.
77. Miralieu E, Vuillez JP, Bardet S, et al. High frequency of bone/bone marrow involvement in advanced medullary thyroid cancer. *J Clin Endocrinol Metab* 2005;90:779–88.
78. Sharkey RM, Karacay H, Chang C-H, et al. Improved therapy of non-Hodgkin's lymphoma xenografts using radionuclides pretargeted with a new anti-CD20 bispecific antibody. *Leukemia* 2005;19:1064–9.
79. Weiden PL, Breitz HB, Press O, et al. Pretargeted radioimmunotherapy (PRIT) for treatment of non-Hodgkin's lymphoma (NHL): initial phase I/II study results. *Cancer Biother Radiopharm* 2000;15:15–29.
80. Forero A, Weiden PL, Vose JM, et al. Phase 1 trial of a novel anti-CD20 fusion protein in pretargeted radioimmunotherapy for B-cell non-Hodgkin lymphoma. *Blood* 2004;104:227–36.
81. Wiseman GA, White CA, Sparks RB, et al. Biodistribution and dosimetry results from a phase III prospectively randomized controlled trial of Zevalin radioimmunotherapy for low-grade, follicular, or transformed B-cell non-Hodgkin's lymphoma. *Crit Rev Oncol Hematol* 2001;39:181–94.
82. Kraeber-Bodere F, Sai-Maurel C, Campion L, et al. Enhanced antitumor activity of combined pretargeted radioimmunotherapy and paclitaxel in medullary thyroid cancer xenograft. *Mol Cancer Ther* 2002;1:267–74.
83. Graves SS, Dearstyne E, Lin Y, et al. Combination therapy with pretarget CC49 radioimmunotherapy and gemcitabine prolongs tumor doubling time in a murine xenograft model of colon cancer more effectively than either monotherapy. *Clin Cancer Res* 2003;9:3712–21.